

BBABIO 43384

## EPR saturation and temperature dependence studies on signals from the oxygen-evolving centre of Photosystem II

R.J. Pace<sup>1</sup>, P. Smith<sup>1</sup>, R. Bramley<sup>2</sup> and D. Stehlik<sup>3</sup>

<sup>1</sup> Chemistry, Department, The Faculties, <sup>2</sup> Research School of Chemistry, Australian National University, Canberra (Australia) and <sup>3</sup> Physics Department, Free University, Berlin (F.R.G.)

(Received 26 July 1990)

(Revised manuscript received 6 February 1991)

Key words: Manganese multiline; Photosystem II; EPR relaxation

Microwave power saturation studies have been performed over the range 4–20 K on EPR signals photogenerated in PS II particles by low-temperature illumination (180–240 K). In the presence of 3% methanol (+MeOH), with no  $g$  4.1 signal present, the multiline signal intensity (extrapolated to zero power) shows strict Curie law behaviour over the 4–20 K range. With no MeOH present in the suspension buffer (–MeOH), both the multiline and 4.1 signals show complementary deviations from Curie law behaviour. These are consistent with the signals arising respectively from the ground,  $S = \frac{1}{2}$ , and first excited  $S = \frac{3}{2}$ , states of a total spin =  $\frac{7}{2}$  multiplet, such as could occur in an MnIV–MnIII antiferromagnetically coupled pair. The deduced height of the  $\frac{3}{2}$  state above the  $\frac{1}{2}$  state is 9.0 K. An inferential estimate, from relaxation data, of this height for the +MeOH case is about 40 K. A broad, featureless component around  $g = 2$  appears to underlie the multiline pattern in the presence of the 4.1 signal, and has a similar temperature behaviour to the latter. A possible exchange coupling model, involving four Mn centres, is presented to accommodate these and other findings on the  $S_2$  state signals.

### Introduction

Photosystem II (PS II) in higher plants is believed to perform the photo-oxidation of  $H_2O$  into  $O_2$  through the action of a manganese containing catalytic site within the membrane-bound protein complex [1]. The reaction proceeds in four one electron steps, each electron feeding to the photo-oxidised reaction centre of PS II (P680) through one or more electron transfer intermediaries. Four relatively stable ( $t_{1/2} > 30$  s at room temperature), kinetically isolatable intermediate states of the manganese centre are known (labelled  $S_0$ – $S_3$ ), each associated with a successive single electron withdrawal [1]. In the dark, the  $S_1$  state is the most stable. Dismukes and Siderer first demonstrated [2] that a characteristic ‘multiline’ EPR signal is associated with

the  $S_2$  state, and Brudvig et al. [3] have shown that this signal may be generated as a single turnover ( $S_1 \rightarrow S_2$ ) by continuous illumination of dark adapted PS II preparations at low temperature (about 200 K). The signal, centred at  $g = 2.0$ , is very similar in its overall features to that seen in bridged, bi-nuclear mixed valence Mn complexes which are antiferromagnetically coupled with a net spin of  $\frac{1}{2}$  [2].

Detailed microwave power saturation studies on the multiline signal have been performed by de Paula and Brudvig [4] on PS II particles and by Hansson et al. [5] on whole chloroplasts. The former investigators found large quantitative differences in multiline relaxation behaviour between samples that had been extensively dark-adapted, prior to freezing and low-temperature illumination, and those which received only a short dark adaptation following multiple turnover by exposure to white light. These treatments were said to produce ‘resting’ and ‘active’ forms of the enzyme, respectively. Quantitation of the intensity appeared to show significant non-Curie behaviour of the resting state signal below about 7 K, the fall-off in amplitude with decreasing temperature being interpreted as population of a state of lower energy than the  $S = \frac{1}{2}$  multiline state.

Abbreviations: EPR, electron paramagnetic resonance; Mes, 2(4-morpholine)ethane sulfonic acid; PPBQ, phenyl *p*-benzoquinone.

Correspondence: R.J. Pace, Chemistry Department, The Faculties, Australian National University, GPO Box 4, Canberra, ACT 2601, Australia.

Such effects were less pronounced or absent in active state forms. Hansson et al. reported Curie behaviour of the multiline signal down to 4 K, but their method of generating the signal (continuous illumination while cooling from 0°C to 77 K) makes direct comparison with the De Paula and Brudvig results difficult. The possible existence of a state below the Kramers  $S = \frac{1}{2}$  multiline state is potentially very interesting, as it would exclude an interpretation of the enzyme  $S_2$  signal in terms of a magnetically isolated bridged manganese pair.

It is now generally believed that a second photo-generated signal, at  $g = 4.1$ , is also associated with the  $S_2$  state in PS II [6,7]. This broad, symmetric signal may be produced on its own by continuous low-temperature (about 140 K) illumination (as originally by Casey and Sauer [8]) or in the presence of some multiline signal by suitable illuminations at higher temperatures (200 K up to about 0°C) which generate the  $S_2$  state in good yield [6,9]. Small hydroxyl-containing molecules (glycerol, ethylene glycol, EtOH, MeOH) inhibit the formation of the 4.1 signal and enhance the multiline signal magnitude [6,10], at least for illumination temperatures above 160 K. These and other results have led to the conclusion that the oxygen-evolving site of PS II in the  $S_2$  state is heterogeneous, with the 4.1 and multiline signals arising from different centres possessing the same basic oxidation state [6,7,10,11].

The temperature dependence of the 4.1 signal has been examined by Brudvig and co-workers [12], who found Curie behaviour in the range 4–20 K. This group has suggested that the 4.1 signal arises from a spin  $\frac{3}{2}$  (ground) state [12,13]. The attractive notion that the 4.1 signal (assuming it is a  $\frac{3}{2}$  state) arises as the first excited state of the species giving rise to the multiline signal is not supported by the recent studies of Hansson et al. [10]. These workers found that the integrated signal intensities in the 4.1 and  $g = 2$  regions (assumed principally to be multiline) showed very similar relative temperature dependences in the range 5–20 K.

In this article we examine in detail the relaxation (power saturation) properties of the multiline and 4.1 signals, both in the presence (no 4.1) and absence of methanol. Signal intensities, extrapolated to zero power, are determined for these species over the temperature range 4–20 K. Unlike the results of Brudvig et al., our data are consistent with the multiline signal arising from a spin- $\frac{1}{2}$  ground state, even for long dark-adapted samples (1–20 h). Further, the temperature dependence of the 4.1 signal strongly suggests that this does not, in our system, arise from a ground state. Complementary deviations from Curie behaviour for both the multiline and 4.1 signals (no MeOH) are quantitatively consistent with these arising from the ground ( $S = \frac{1}{2}$ ) and first excited states ( $S = \frac{3}{2}$ ), respectively, of an antiferromagnetically exchange coupled  $S = \frac{7}{2}$  multiplet. However,

our data are not necessarily in conflict with those of Hansson et al. [10] as we find evidence for a broad resonance at  $g \approx 2$  which appears to underly the multiline in the presence of the 4.1 signal. This  $g \approx 2$  signal contributes substantially to the total integrated intensity around  $g \approx 2$  and has a similar (non-Curie) temperature dependence to the 4.1 signal.

## Materials and Methods

PS II particles derived from spinach were used exclusively. The spinach was greenhouse grown and freshly picked in the morning prior to particle preparation that day. Particles were made from chloroplasts following the method of Bricker et al. [14], replacing the proteinase inhibitor in the blendate and first wash with high levels of bovine serum albumin and omitting the

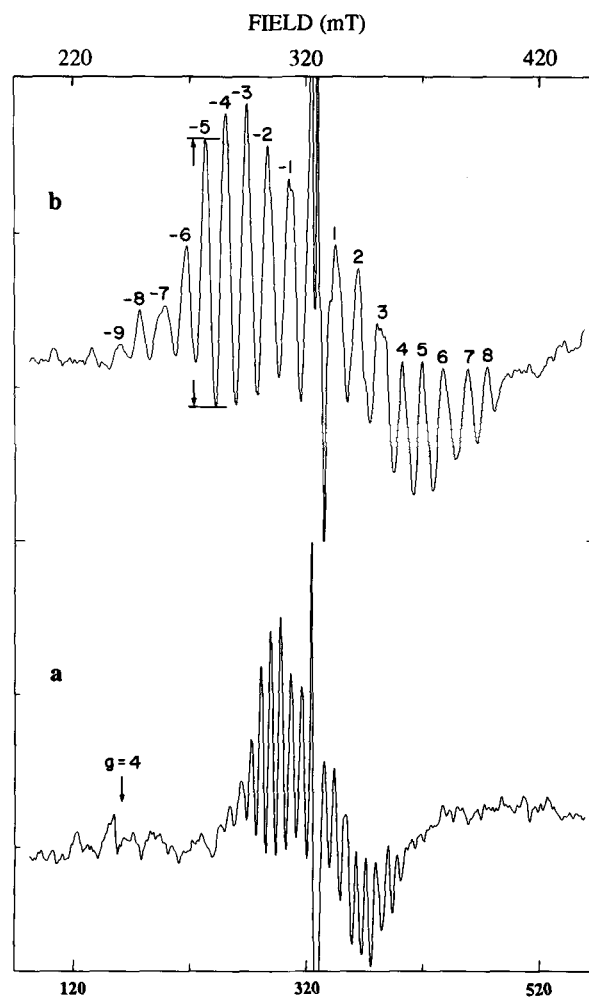


Fig. 1. (a) Illuminated (220 K) minus dark spectrum for +MeOH sample (see text). The  $g = 4.0$  point is indicated. Scan width is 500 mT. (b) Expanded scan of multiline region showing line numbering scheme used here. Peak heights were estimated as indicated. Each trace is the average of two scans. Spectrometer conditions: 9.03 GHz, 20 G peak-to-peak field modulation amplitude, 30 mW power, 100 kHz field modulation frequency, temperature 8.0 K, scan width 250 mT.

divalent cation wash step. The material was suspended at about 15 mg Chl/ml in a storage buffer containing 20 mM Mes (pH 6.0, HCl), 10 mM  $\text{MgCl}_2$ , 15 mM NaCl and 400 mM sucrose and frozen in liquid nitrogen. As made, the material showed an oxygen-evolving activity in the range 500–1100  $\mu\text{mol O}_2/\text{mg Chl per h}$ , using PPBQ and  $\text{Fe}(\text{CN})_6^{3-}$  as electron acceptors in 10 mM  $\text{Cl}^-/\text{medium}$ .

Freshly thawed material (13–16 mg/ml Chl) was used for each experiment and retained on ice for 1–20 h in the dark prior to making up the EPR samples. These were made by diluting concentrated stocks of EDTA and DCMU (in dimethyl sulphoxide) or pure methanol into aliquots of PS II in storage buffer, to give final concentrations of 1.5 mM, 100  $\mu\text{M}$  or 3%, respectively. Following a 5 min equilibration at room temperature, the samples (in 3 mm quartz capillaries) were cooled to the illumination temperature (180–240 K) in a nitrogen flow cryostat and illuminated for 4 min with strong green light ( $150 \text{ W m}^{-2}$ ). The samples were then quickly frozen to 77 K before loading into the spectrometer cavity.

EPR measurements were performed on a Varian V-4502 X-band spectrometer, equipped with an Oxford ESR9 helium flow cryostat. This was run at high He flow rates (about 2.5 l/h) and calibrated by a carbon resistor in the sample position. Temperature uncertainty in the sample is estimated as about 0.3 K. Spectra were recorded on a computer data logging system interfaced to the spectrometer. The microwave power entering the cavity was measured with a Hewlett Packard 435A power meter.

## Results

### Plus MeOH samples

Fig. 1a shows a typical illuminated-minus-dark spectrum for PS II particles with 3% MeOH in the buffer medium (+MeOH). We consistently see under these conditions an 18 line pattern (one line obscured in the  $g = 2$  region), with no significant intensity in the  $g = 4$  region. Fig. 1b shows an expanded scan of the multiline pattern with the indicated line numbering used here. Small features to lower field than -9 are variable and

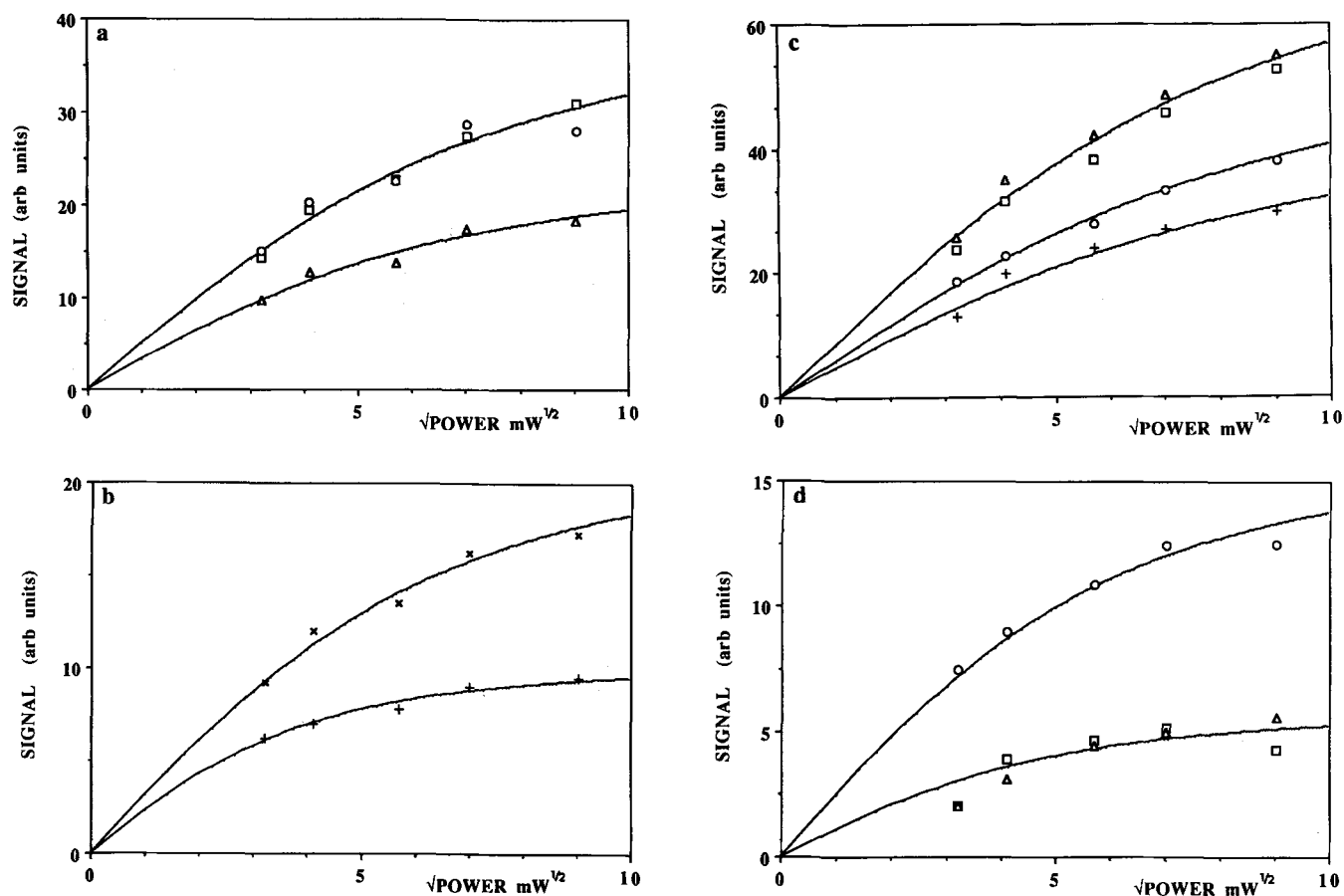


Fig. 2. Power saturation plots of individual peaks in the +MeOH multiline spectrum at 8 K. (a) Upfield peaks; 4,  $\square$ , 5,  $\circ$  (69 mW); 6,  $\triangle$  (53 mW). (b) 7,  $\times$  (51 mW); 8,  $+$  (20 mW). (c) Downfield peaks; -5,  $\triangle$ , -3,  $\square$ , (80 mW); -2,  $\circ$  (90 mW); -6,  $+$  (88 mW). (d) -7,  $\circ$  (44 mW); -8,  $\square$ ; -9,  $\triangle$  (29 mW). Figures in brackets are  $P_{1/2}$  values.

in general line -9 is discernible only under favourable (high signal/noise) conditions. Individual line intensities were estimated in the conventional way as shown in Fig. 1b.

Fig. 2 shows power saturation plots of the individual lines at 8 K. The behaviour is reasonably symmetric around  $g = 2$ , with the three most downfield and up-field lines showing similar microwave power response. These lines saturate more readily than do the intervening peaks, all of which appear to show similar saturation behaviour amongst themselves.

The separate hyperfine lines are of course only partly resolved, especially towards the middle of the pattern, making application of a simple saturation analysis problematic. However, each line is certainly inhomogeneously broadened and so we adopt as an approximation an interpretation based on a single inhomoge-

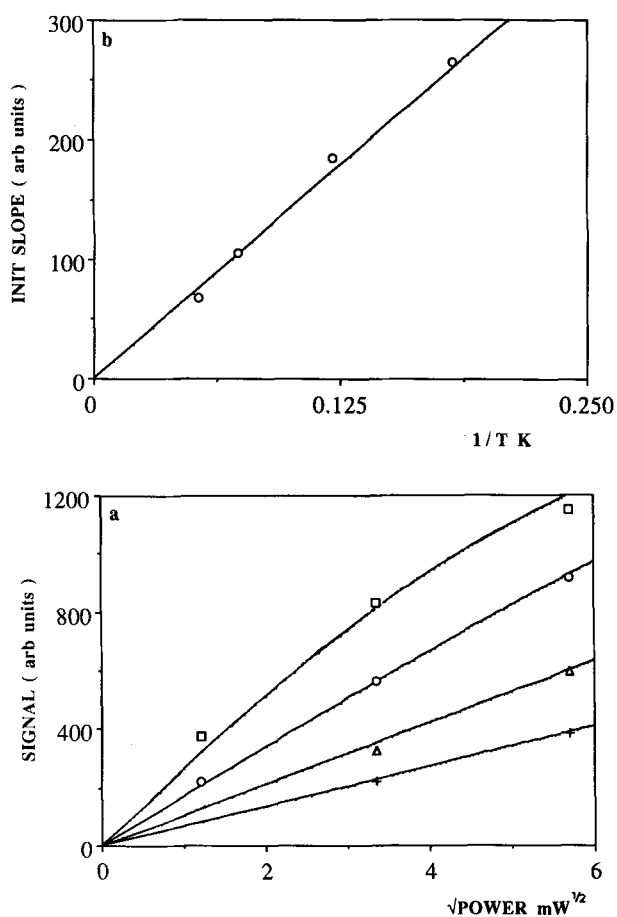


Fig. 3. (a) Power saturation plots for the +MeOH multiline signal intensity over the range 5–18 K. Signal estimated as sum of peak heights from downfield peaks -6, -5, -4, -3, -2, as indicated in Fig. 1. The curves are fits to the data of equation 1 (see text). Temperature points are: □, 5.5 K; ○, 8.3 K; △, 13.7 K; +, 18.3 K. (b) Curie plot of the fitted  $C$  parameters (initial slopes, see text) from the data in (a).

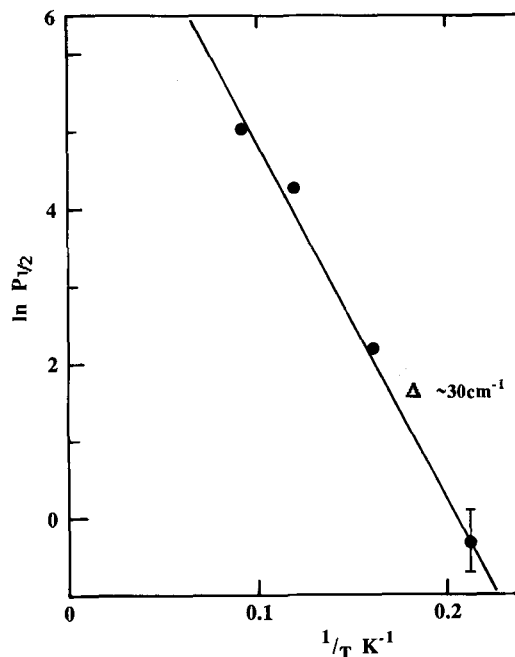


Fig. 4. Plot of  $\ln P_{1/2}$  against inverse temperature for +MeOH sample, over the range 4.7 to 11 K. The  $P_{1/2}$  values were determined by fitting data such as in Fig. 3 to Eqn. 1. The slope corresponds to an energy gap ( $\Delta$ ) in an Orbach process of  $30 \text{ cm}^{-1}$  (see text).

neously broadened line [15]. Hence, each data set was fitted with a curve of the form,

$$S(\text{signal}) = C\sqrt{P} / \sqrt{(1 + P/P_{1/2})} \quad (1)$$

Here  $P_{1/2}$  is the half-saturation power, proportional to the product of the longitudinal and transverse relaxation rates and  $C$  is a measure of the 'true' signal intensity in the low power limit, where  $S = C\sqrt{P}$  rigorously. The  $P_{1/2}$  values are indicated in the figure caption and the wing lines are seen to have values about half those of the intervening lines.

Fig. 3a shows root power saturation plots, at various temperatures, of the multiline signal amplitude estimated as the sum of the heights of the five prominent downfield peaks (-6... -2). These were chosen on the basis of homogeneity of saturation behaviour, ease of detection and freedom from underlying or adjacent signals. The corresponding Curie plot of the fitted  $C$  parameters (initial slopes) are shown in Fig. 3b. There is no significant deviation from linearity in the range 5–20 K that we are able to detect. This behaviour was consistently seen for samples extensively dark adapted on ice (1–20 h) and the data in Fig. 3 are from material given a 20 h dark-adaption. At microwave powers available in our instrument (up to about 160 mW), deviations from linearity on the saturation plots are detectable up to about 12 K. Fig. 4 shows a plot of the inferred  $\ln P_{1/2}$  versus  $1/T$  values for  $T$  between 4.7 and 11 K.

If the relaxation is assumed to arise from an Orbach process (Ref. 16) operating on  $T_1$ , the slope of the plot in Fig. 4 suggests a  $\Delta$  value of about  $30 \text{ cm}^{-1}$  (see Discussion). This is very similar to the value,  $\Delta \approx 29 \text{ cm}^{-1}$ , determined by Hansson et al. on whole chloroplasts.

#### Minus MeOH samples

Fig. 5a shows a typical illuminated-minus-dark spectrum for PS II particles with the -MeOH buffer medium. The PS II particles were dark adapted at  $0^\circ\text{C}$  for more than 1 h prior to illumination. For illumination temperatures of about 180–260 K (with DCMU in DMSO added above 220 K to prevent advancement beyond  $S_2$ ) we see essentially the same results, a mixture of 4.1 and multiline signals of roughly comparable intensities. Although we find that the multiline to 4.1 signal ratio declines somewhat with decreasing illumination temperature in the above range, we are unable to produce

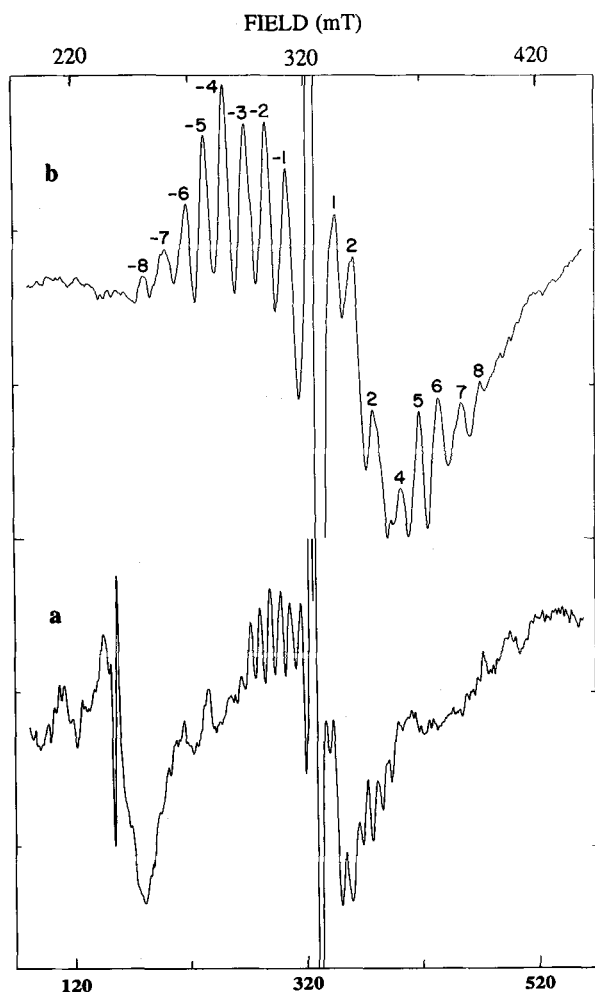


Fig. 5. (a) Illuminated (200 K) minus dark spectrum for -MeOH sample (see text). Both the 4.1 and multiline signals are apparent. (b) Expanded scan of multiline region showing line numbering. This is equivalent to that shown in Fig. 1 for the +MeOH sample. Average of two scans; spectrometer conditions as in Fig. 1 for (a) and (b).

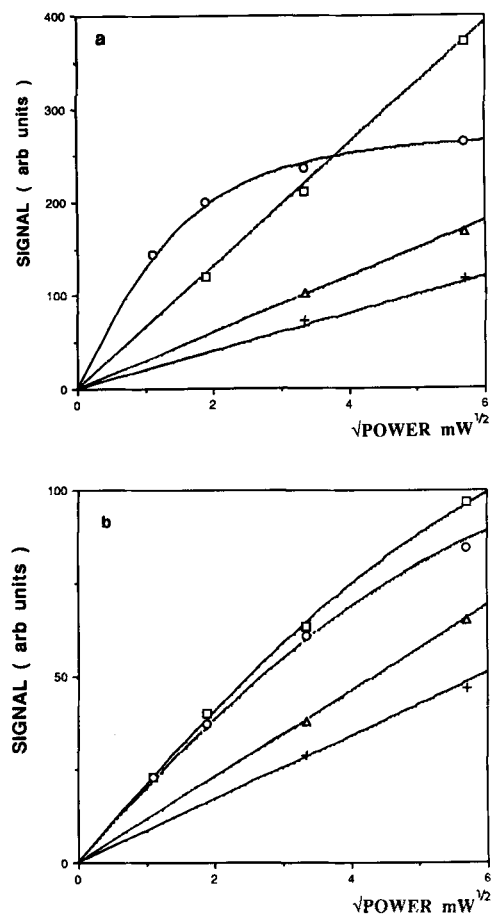


Fig. 6. Power saturation plots for the amplitudes of the (a) -MeOH multiline signal (sum of the heights of downfield peaks -2, -3, -4, -5, -6) and (b) 4.1 signal (peak to peak) over the temperature range 4.7–17.1 K. The curves are fits to Eqn. 1 (see text). Temperature points are:  $\circ$ , 4.7 K;  $\square$ , 8.3 K;  $\triangle$ , 13.9 K;  $+$ , 17.1 K.

detectable levels of 4.1 signal alone by 140 K illumination as reported by others [8,11]. We suspect this is a cryoprotectant-related effect (see Discussion), but have not pursued a detailed study along these lines.

Fig. 5b shows an expanded scan of the multiline pattern. A line numbering similar to that employed for the +MeOH samples is indicated. In the downfield region, the + and -MeOH patterns are quite similar, but the existence of a -9 line in the -MeOH sample is uncertain. Upfield, the two patterns are less similar, although this may be in part due to differences in the  $g \approx 1.9$ – $1.8$  FeQ signal region. One evident feature on comparing Figs. 1 and 5 is the apparent existence of a broad, roughly gaussian signal entered around  $g \approx 2$  underlying the multiline in the -MeOH spectrum. Little, if any such 'signal' is obvious in the +MeOH spectrum. The possible existence of such a feature has been noted previously [5,9,12], but no consensus seems to have emerged as to its origin.

The relative relaxation behaviour across the -MeOH pattern is generally similar to that seen for the +MeOH

pattern (Pace et al., unpublished data) but the significantly lower signal intensity and proportionately smaller wing lines makes a detailed analysis such as in Fig. 2 unreliable. However, the signal amplitude may be readily estimated from the same five downfield peaks used above. Similarly, the  $g = 4.1$  signal amplitude may be taken as proportional to the peak-to-peak height, as the line shape is temperature-independent in the range of interest here (see below). Fig. 6 shows root power saturation plots for the multiline (a) and 4.1 signals (b), respectively, quantitated as above. Fig. 7 shows the corresponding Curie plots of the fitted initial slopes from Fig. 6. Representative error bars corresponding to the estimated uncertainties in both temperatures and signal magnitudes are indicated. Both data sets show complementary deviations from Curie behaviour that we believe to be outside experimental uncertainty. The curves are theoretical fits discussed below.

These results differ qualitatively from earlier reported behaviour of the multiline and 4.1 signals. The deviation from linearity that we observe for the multiline signal is concave up, rather than concave down as reported by Brudvig and co-workers [4,12] over a similar temperature interval (4–20 K). Moreover, we see unambiguous non-Curie behaviour of the 4.1 signal (concave down), unlike these authors (see Discussion,

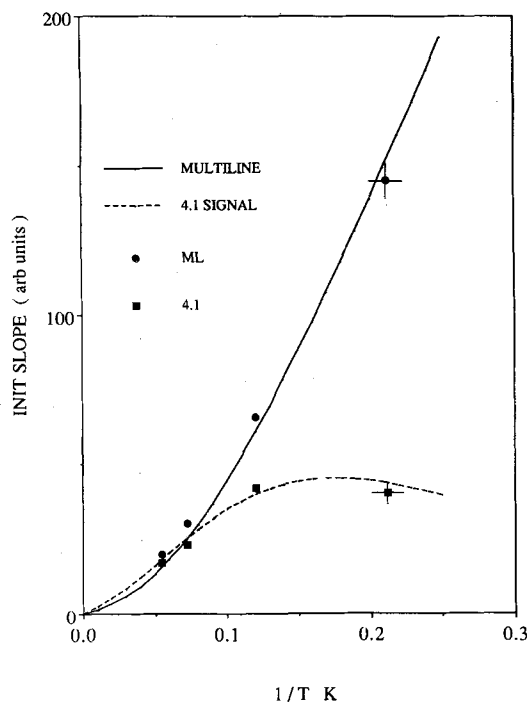


Fig. 7. Curie plots of the fitted  $C$  parameters (or measured linear slopes where appropriate) for the multiline (●) and 4.1 (■) signals from the data in Fig. 6. The curves are fits of both data sets to Eqn. 4 (see text), assuming  $S = \frac{1}{2}$  for the multiline signal,  $S = \frac{3}{2}$  for the 4.1 signal and  $J = -3.0$  K. The  $I_{0s}$  values have no relative significance (due to the method of signal quantitation) and are 940 and 453 arb. units for the multiline and 4.1 signals respectively.

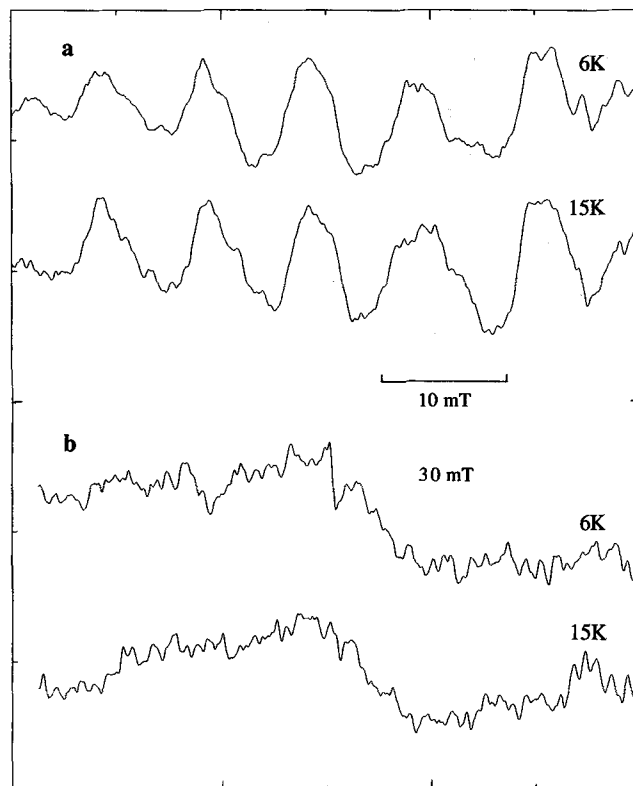


Fig. 8. Detailed line shapes for the five multiline downfield peaks (a) and 4.1 signal (b) used for signal quantitation in -MeOH samples at 6 K and 15 K. Spectrometer conditions as in Fig. 1, and as used to obtain the data in Fig. 6. The same basic line detail is resolved at both temperatures in (a) and there is no discernible line broadening in (b).

however, for further examination of this point). In addition, we would clearly infer a strong temperature dependence in the ratio of the multiline: 4.1 signal intensities, in the range 4–20 K, unlike Hansson et al. [10], who report little such variation. Given these discrepancies, it is important to identify any artefacts, etc., that may be contributing to the analysis. We regard our method of signal quantitation, (taking the initial slopes of  $\sqrt{P}$  plots) to be more reliable than intensity measurements at fixed (low) powers which are presumed to be in the non saturation regime. This is particularly so when  $P_{\frac{1}{2}}$  varies rapidly with temperature, as for the multiline signal. A greater concern is that linewidth variation with temperature may invalidate our method of signal quantitation. This is most unlikely for the 4.1 signal, as our data (Fig. 8b) and those of Hansson et al. [10] show no significant variation of signal shape (derivative or absorption) over the range 5–20 K. Although previous workers have generally quantitated the multiline signal by summed heights of selected peaks, as here, Hansson et al. [10] have raised the possibility that this is invalid. These authors inferred an increase in intrinsic linewidth, with increasing temperature, particularly for non-alcohol-containing samples. This derived from a comparison of individual peak heights and the overall

pattern envelope amplitude, as per Hyde and Subczynski [17]. This analysis is itself invalid, of course, if signals other than the multiline contribute to the envelope amplitude.

It is well known that the individual peaks in the multiline pattern show a resolved super hyperfine structure, whose origin is presently unclear. Fig 8a shows a comparison, under non-saturating conditions, of the detailed downfield peak structures seen at low (6 K) and high (15 K) temperatures. Spectrometer conditions were the same as those employed in the signal quantitation studies. Although there are slight alterations in some peak shapes, there is no significant evidence of homogeneous peak broadening or change in resolved structure at the high temperature. Virtually all of the regions of rapid shape discontinuity (sharp edges, etc.) seen at the lower temperature are seen also at the higher

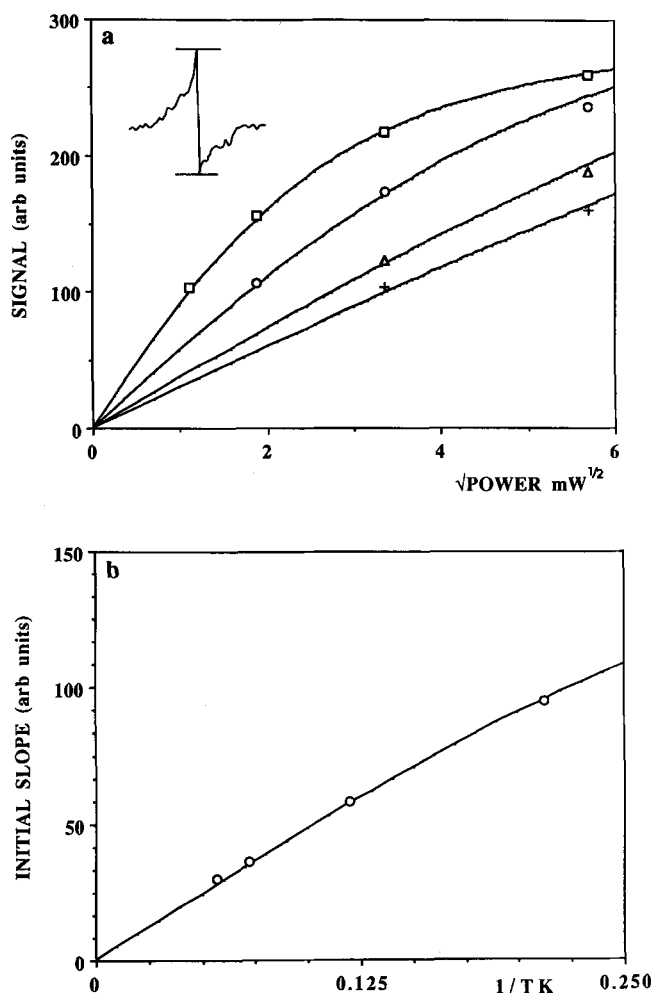


Fig. 9. (a) Power saturation plots for the amplitude of the rhombic iron,  $g = 4.3$  signal from dark-adapted PS II membranes, over the temperature range 4.7–17 K. Curves are fits of Eqn. 1 to data (see text). Signal was quantitated as peak-to-peak amplitude, as indicated in inset. Temperature points are:  $\square$ , 4.7 K;  $\circ$ , 8.3 K;  $\triangle$ , 13.9 K;  $+$ , 17.1 K. (b) Curie plot of the fitted  $C$  parameters from data in (a). Curve is theoretical fit of the expression  $S = S_0/T[e^{-\theta/T}/(1 + e^{-\theta/T} + e^{-2\theta/T})]$ , with  $S_0 = 1480$  arb. units and  $\theta = 2.6$  K (see text).

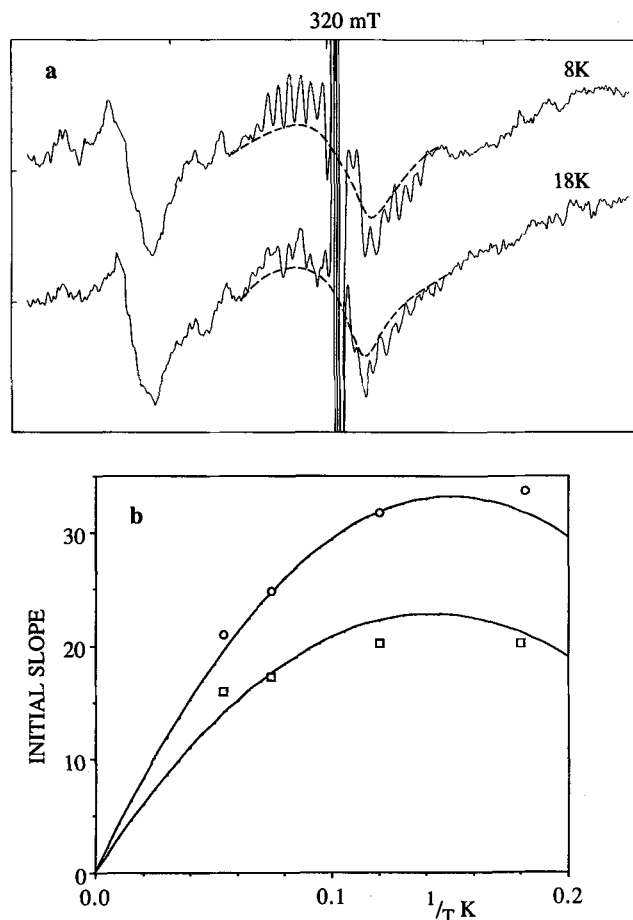


Fig. 10. (a) Illuminated (200 K) minus dark spectra for  $-\text{MeOH}$  sample at 8 K and 18 K, showing the estimated shape of the putative broad underlying component. This is of comparable size for the two temperatures, although the multiline signal is substantially diminished at 18 K relative to 8 K. Spectrometer conditions as in Fig. 1. (b) Curie plots of the 4.1 ( $\circ$ ) and broad  $g \approx 2$  ( $\square$ ) signals from the same sample, obtained from power saturation analyses as used in Fig. 9, etc. Temperature range 5–18 K.

temperature. We thus conclude that any variation in intrinsic linewidth is less than the field modulation amplitude (20 G) used here, and that our method of signal quantitation is not compromised by linewidth effects.

Finally, there is a convenient internal 'standard' on which we may test our methods of analysis. This is the inorganic ('junk') iron,  $g = 4.3$  signal always present to some degree in PS II preparations. This isotropic signal at  $g = 4.29$  has been shown to arise uniquely from  $\text{Fe}^{3+}$  in a purely rhombic environment ( $D = 0$ ,  $E > 0$ , Ref. 18), here presumably hydrated  $\text{Fe}_2\text{O}_3$  from cytochrome degradation, etc. The zero-field ground states consist of three equally spaced degenerate (Kramers) doublets, of separation  $\theta \approx 2.6$  K between doublets. The centre doublet gives rise to the 4.29 signal in a magnetic field. Fig. 9a shows amplitude versus root power plots for the 4.29 signal in a long dark adapted sample (no 4.1). The signal shape was found to be temperature-independent

and the intensity was measured as peak height, as for the multiline and 4.1 species, as indicated in the inset. Fig. 9b shows the corresponding Curie plot. This should exhibit a slight downward curvature in the range 4–20 K, as the 4.29 signal arises from the centre state. The curve is a fit assuming  $\theta = 2.6$  K, as indicated in the figure. The agreement would appear to exclude any instrumental artefacts occurring in our measurements.

The above results suggest that there may indeed be a broad component under the multiline in the presence of the 4.1 signal. This is evident from the examples in Fig. 10a, showing a comparison of spectra (non-saturating conditions) at 8 and 18 K from a sample illuminated at 200 K. An estimate of the shape of the putative broad signal is indicated by the dashed lines, drawn to just underlie the multiline peaks. This is rough but adequate for our purposes. It seems implausible, particularly at the higher temperature, that the overall multiline pattern shape arises simply from peak overlapping due to the intrinsic line width. Indeed, simulations (Pace et al., unpublished data) show that if this were indeed so, no superhyperfine structure, such as seen in Fig. 8a, would be resolvable. Fig. 10b shows Curie plots of the 4.1 and broad  $g \approx 2$  signals from the same sample derived from signal versus  $\sqrt{P}$  data in the usual manner. The Curie plots confirm the impression already evident from Fig. 10a that the 4.1 and broad  $g \approx 2$  signals have a similar, non Curie, temperature dependence. It is also obvious from Fig. 10, that the ratio of the *integrated* total signal intensities in the 4.1 and multiline regions would vary only weakly with temperature in the range 4–20 K (and this is indeed so). Hence, our data are not in conflict with those of Hansson et al. [10], who employed such an analysis.

## Discussion

The results obtained here strongly suggest that the  $S = \frac{1}{2}$  multiline state, formed either in the presence or absence of the 4.1 signal, is a ground doublet. We see no deviations from Curie behaviour for this signal that would suggest the existence of a lower, thermally accessible spin state. This is in conflict with the results of De Paula et al. [4,12] but consistent with the data of Hansson et al. [5,10]. This latter group claims to have eliminated differences in sample preparation (essentially the cryoprotectant used) as a cause of the discrepancy [10].

The deviation from Curie behaviour that we do observe for the multiline signal in the presence of the 4.1 signal suggests the existence of a thermally accessible state, about 10 K above the  $S = \frac{1}{2}$  multiline state. Further, the 4.1 signal shows a complementary deviation from Curie behaviour and is commonly supposed to derive from a quasi-axial,  $S = \frac{3}{2}$  state. Given that a minimal model for the multiline centre is an antiferro-

magnetically coupled Mn hetero-dimer (MnIV-MnIII or MnIII-MnII, Ref. 1, with MnIV-MnIII being preferred), it is tempting to identify the multiline and 4.1 signals with the ground ( $S = \frac{1}{2}$ ) and first excited ( $S = \frac{3}{2}$ ) states of a coupled MnIV-MnIII,  $S = \frac{7}{2}$  multiplet. If the exchange Hamiltonian has the form:

$$\mathcal{H} = -2JS_1 \cdot S_2 (S_1 = 2, S_2 = \frac{3}{2}) \quad (2)$$

then the energy levels are given by

$$E_s/J = S_1(S_1 + 1) + S_2(S_2 + 1) - S(S + 1) \quad (3)$$

where  $S$ , the total spin, takes values  $\frac{1}{2} \dots \frac{7}{2}$ .

At thermal equilibrium, the relative intensities ( $I$ ) of EPR transitions arising from the various spin states are then,

$$I_s = \frac{I_{os}}{T} \left[ \frac{(2S+1) e^{-E_s/kT}}{\sum_j (2j+1) e^{-E_j/kT}} \right] j = \frac{1}{2} \dots \frac{7}{2} \quad (4)$$

The bracketed expression in Eqn. 4 is the Boltzmann factor and the remainder the Curie term. The  $I_{os}$  constants depend on the transition probability for each state, as well as the total spin concentration etc. and are not known here. The curves in Fig. 7 were drawn assuming that  $J = -3.0$  K and the multiline and 4.1 signals arise from the  $S = \frac{1}{2}$  and  $\frac{3}{2}$  states, respectively (energy gap = 3 J), with the  $I_{os}$  terms as free parameters. The observed deviations from Curie behaviour of both signals are well reproduced. Assuming, as seems reasonable, that a similar basic model obtains for the multiline centre in the presence of MeOH, then the apparent Curie behaviour of the multiline signal seen in Fig. 3b would suggest a value of  $|J| > 10$  K. This would be consistent with the interpretation that the temperature dependence of  $P_{\frac{1}{2}}$  in Fig. 4 reflects an Orbach process, with the  $T_1$  relaxation pathway going through the first accessible ( $S = \frac{3}{2}$ ) excited state. The inferred value of  $J$  would be  $-\Delta/3$  (approx.  $-13$  K). This estimate is, however, far more inferential than that from Fig. 7.

Interestingly, the relatively very weak temperature dependence of  $P_{\frac{1}{2}}$  for the 4.1 signal seen in Fig. 6 is then consistent with this signal arising from a thermally excited state, as suggested above, and the relaxation occurring by a 'reverse' Orbach process through the ground state (multiline state). The transition probability for such a 'de-excitation' pathway would not be expected to show a strong temperature dependence over a limited range of  $T$  (say, 5–10 K). All common relaxation mechanisms operating on ground state metal centres seem to show at least a  $T^n$  ( $n > 2$ ) dependence for temperatures below about 100 K [15]. Notice also the weak temperature dependence of  $P_{\frac{1}{2}}$  for the rhombic



iron signal in Fig. 9, where this signal also arises from an excited state.

Taken together, our data would support the view that there actually is a broad, quasi gaussian photo-generated component around  $g \approx 2$  underlying the multiline signal. In our hands, this feature is associated with the 4.1 signal and has a similar, non Curie behaviour. It has been previously suggested that this supposed gaussian 'signal' is not real, being merely a consequence of line overlapping due to  $g$  anisotropy [12] or line broadening [10]. The Q-band results in Ref. 10 would appear to exclude any significant  $g$  anisotropy in the multiline signal. Similarly, we observe no evidence of homogeneous line width contributions sufficient to account for the apparent existence of a broad component. Moreover, the temperature dependences of the resolved multiline and broad components differ substantially, making it unlikely that inhomogeneous effects, such as hyperfine anisotropy, are responsible.

Although our data are quantitatively consistent with the simple notion that the multiline and 4.1 signals arise from the first two spin states of an antiferromagnetically coupled Mn heterodimer (probably MnIV-MnIII), there are problems with this interpretation. Firstly, it is well known that under a range of conditions the 4.1 signal appears to be a ground state, i.e., may be generated essentially in the absence of resolved multiline [8,13,19]. These conditions generally involve low ( $\leq 140$  K) temperature illumination and/or alterations in the optimum buffer electrolyte regime ( $\text{Cl}^-$  depletion,  $\text{NH}_4\text{Cl}$  treatment, etc.). Subsequent annealing of the sample at higher temperature ( $\geq 200$  K) in some cases allows formation of multiline at the expense of 4.1 signal [8,13]. A second difficulty with the above heterodimer interpretation of the  $S_2$  state signals is that it does not obviously admit the broad  $g \approx 2$  signal.

To accommodate these observations, it seems necessary to invoke additional magnetic interactions. EXAFS studies [20], as well as the +MeOH type of multiline behaviour strongly suggest that a bridged hetero dimer is an appropriate model for at least two of the 4 Mn known to be present in the fully functional complex. Moreover, the overall manganese oxidation state of the  $S_2$  form appears to be the same, irrespective of whether the 4.1 or multiline species is present [7] on illumination. Consider a scheme for the  $S_2$  state such as shown in Fig. 11. This envisages a tightly coupled MnIV-III dimer ( $J_1$ ), which then interacts by a coupling of variable magnitude ( $J_2$ ) with an MnIII, which itself may interact with a further MnIII ( $J_3$ ). All couplings are antiferromagnetic, with one possible exception (see below). Most of the behaviour discussed above may then be formally reproduced by varying the magnitudes of  $J_2$  and  $J_3$ , while retaining  $J_1$  fixed. The multiline ( $S_T = \frac{1}{2}$ ) is always a ground state arising from the IV-III dimer, effectively in isolation, either because it is not coupled

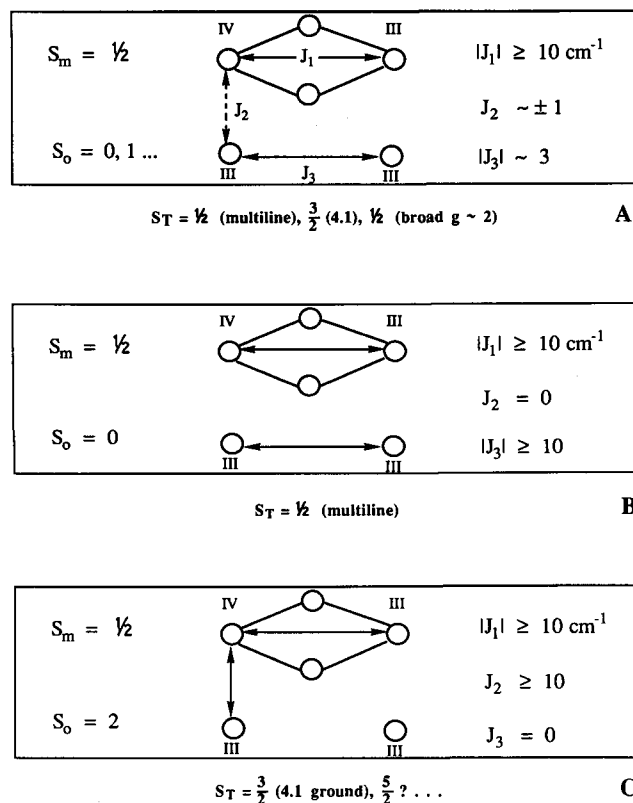


Fig. 11. Possible scheme for magnetic interactions between the 4 Mn atoms in the  $S_2$  state of the oxygen-evolving complex. (A) -MeOH form displaying multiline, 4.1 and broad  $g \approx 2$  signals (non Curie behaviour); (B) +MeOH form displaying Curie multiline behaviour (no 4.1); (C) low-temperature illumination form showing no multiline but ground state 4.1 behaviour.

to other spins (+ MeOH) or coupled to a state of zero spin (- MeOH). In the latter case, the 4.1 ( $S_T = \frac{3}{2}$ ) arises from coupling (through  $J_2$ ) of the dimer  $S_m = \frac{1}{2}$  state to the first excited ( $S_0 = 1$ ) state of the other Mn pair. This also produces an 'excited'  $S_T = \frac{1}{2}$  state (broad  $g \approx 2$ ) of similar temperature dependence to the 4.1 state if  $|J_2|$  is small ( $\leq 1 \text{ cm}$ ; note that in this instance  $J_2$  may be positive or negative and still consistent with the data). The multiline and 4.1/ $g \approx 2$  states will have complementary, non Curie behaviour (over our observation range), with an apparent energy gap determined largely by  $J_3$ . Reduced hyperfine couplings and overlapping lines might make the 4.1 and  $g \approx 2$  states featureless. If  $J_2$  strengthens and  $J_3$  weakens to  $\approx 0$ , then the IV-III dimer is coupled to a single MnIII. This would produce an  $S_T = \frac{3}{2}$  (4.1 type) ground state, in the absence of a multiline signal. Since Brudvig et al. [11-13] typically generate such a 4.1 signal by low temperature ( $\approx 130$  K) illumination, their observation of Curie behaviour for this species may not be inconsistent with the arguments developed here.

Interestingly,  $J_2$  and  $J_3$  must vary at each others' expense to produce the full range of behaviours seen above. This might represent only small movements

within the protein matrix, as all the posited exchange interactions are relatively weak compared to model Mn bridged dimer systems [21]. Whether the scheme shown in Fig. 11 represents some approximation of the magnetic structure actually existing within the oxygen evolving complex, only future studies will resolve. However, one prediction is clear. The multiline state arises from what may be regarded essentially as an isolated, bridged Mn heterodimer. The small lines seen in the wings of the pattern, beyond the 16 expected from model compound studies, do not then arise from interactions with additional Mn centres. Presumably, they would be a consequence within the powder pattern of significant hyperfine anisotropy at one or both Mn atoms. The somewhat different relaxation behaviour of the outer lines, seen in Fig. 2, might also be a reflection of this fact.

## References

- 1 Dismukes, G.C. (1986) *Photochem. Photobiol.* 43, 99–115.
- 2 Dismukes, G.C. and Siderer, Y. (1981) *Proc. Natl. Acad. Sci. USA* 78, 274–278.
- 3 Brudvig, G.W., Casey, J. and Sauer, K. (1983) *Biochim. Biophys. Acta* 723, 366–371.
- 4 De Paula, J.C. and Brudvig, G.W. (1985) *J. Am. Chem. Soc.* 107, 2643–2648.
- 5 Hansson, O., Andreasson, L.-E. and Vänngård, T. (1984) in *Advances in Photosynthesis Research*, Vol. 1 (Sybesma, C., ed.), pp. 307–310, Nijhoff/Junk, Dordrecht.
- 6 Zimmermann, J.-L. and Rutherford, A.W. (1986) *Biochemistry* 25, 4609–4615.
- 7 Cole, J., Yachandra, V.K., Guiles, R.D., McDermott, A.E., Britt, R.D., Dexheimer, S.L., Sauer, K. and Klein, M.P. (1987) *Biochim. Biophys. Acta* 890, 395–398.
- 8 Casey, J.L. and Sauer, K. (1984) *Biochim. Biophys. Acta* 767, 21–28.
- 9 Zimmermann, J.-L. and Rutherford, A.W. (1984) *Biochim. Biophys. Acta* 767, 160–167.
- 10 Hansson, O., Aasa, R. and Vänngård, T. (1987) *Biophys. J.* 51, 825–832.
- 11 De Paula, J.C., Innes, J.B. and Brudvig, G.W. (1985) *Biochemistry* 24, 8114–8120.
- 12 De Paula, J.C., Beck, W.F. and Brudvig, G.W. (1986) *J. Am. Chem. Soc.* 108, 4002–4009.
- 13 Beck, W.F. and Brudvig, G.W. (1986) *Biochemistry* 25, 6479–6486.
- 14 Bricker, T.M., Pakrasi, H.B. and Sherman, L.A. (1985) *Arch. Biochem. Biophys.* 237, 170–176.
- 15 Castner, T.G., Jr. (1959) *Physiol. Rev. Ser. 2*, 115, 1506–1515.
- 16 Abragam, A. and Bleaney, B. (1970) *Electron Paramagnetic Resonance of Transition Ions* Ch. 10, Oxford University Press, Oxford.
- 17 Hyde, J.S. and Subczynski (1984) *J. Magn. Res.* 56, 125–130.
- 18 Castner, T., Jr., Newell, G.S., Holton, W.C. and Slichter, C.P. (1960) *J. Chem. Phys.* 32, 668–673.
- 19 Ono, T., Zimmermann, J.L., Inoue, Y. and Rutherford, A.W. (1986) *Biochim. Biophys. Acta* 851, 193–201.
- 20 Yachandra, V.K., Guiles, R.D., McDermott, A.E., Cole, J.L., Britt, R.D., Dexheimer, S.L., Sauer, K. and Klein, M.P. (1987) *Biochemistry* 26, 5974–5981.
- 21 Inoue, M. (1978) *Bull. Chem. Soc. Jpn.* 51, 1400–1403.